PROCEEDINGS OF SCIENCE

$B_d \to K^{*0}\mu^+\mu^-$ at LHC*b*

William Reece[*†]
*(on behalf of the LHC*b *collaboration)*
E-mail: w.reece06@imperial.ac.uk

$\bar{B}_d \to \bar{K}^{*0}\mu^+\mu^-$ is a rare electroweak $b \to s$ penguin decay that has excellent sensitivity to physics beyond the Standard Model. LHC*b* should collect $6200\ ^{+1700}_{-1500}$ signal events with a residual background of 1550 ± 310 for each nominal year of data taking. This allows for a comprehensive and exciting programme of physics measurements, the details of which will be reviewed in this article.

12th International Conference on B-Physics at Hadron Machines - BEAUTY 2009
September 07 - 11 2009
Heidelberg, Germany

[*]Speaker.
[†]Imperial College London

PoS(BEAUTY 2009)051

1. Introduction

As we enter the LHC era, we are confronted with the experimental fact that results from the TeVatron and the *B*-factories are, by and large, in agreement with Standard Model (SM) predictions. The working hypothesis of the LHC project is that there will be new physics (NP) at the TeV scale. However, considerations from flavour physics imply that the NP scale is much larger, assuming its flavour structure is generic. If these two observations are to be reconciled then the study of flavour will be of great interest at the LHC.

LHC*b* is a high precision experiment for the study of *CP*-violation and rare decays at the LHC [1]. Of particular interest will be the exclusive $b \to s$ decay mode $\bar{B}_d \to \bar{K}^{*0}\mu^+\mu^-$. This is normally treated using the operator product expansion, where the Wilson coefficients $\mathscr{C}_{7,9,10}$ dominate [2]. These have right-handed partners, $\mathscr{C}'_{7,9,10}$, that are highly suppressed in the SM and in minimal flavour-violating models [3]. In the presence of NP, the values of these coefficients may change due to new heavy degrees of freedom in the loops. Measuring the Wilson coefficients then allows for entire classes of NP to be observed or excluded.

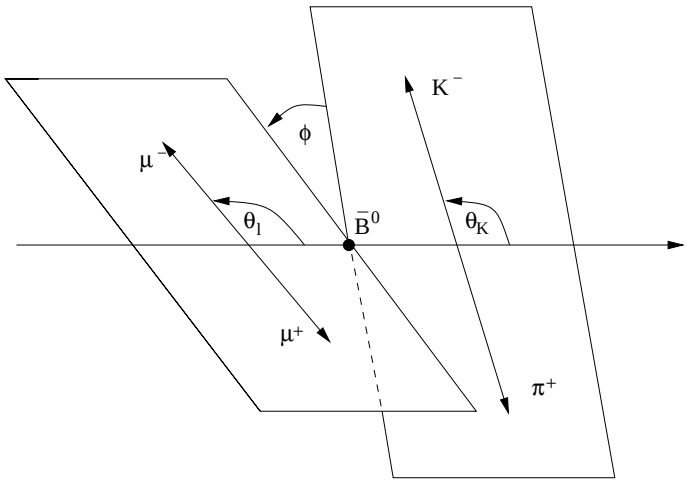

Figure 1: Definition of kinematic variables in the decay $\bar{B}_d \to \bar{K}^{*0}\mu^+\mu^-$ (e.g. Ref. [4]): The z-axis is the direction in which the $\bar{B}$ meson flies in the rest frame of the $\mu^+\mu^-$. θ_l is the angle between the μ^- and the z-axis in the $\mu^+\mu^-$ rest frame, θ_K is the angle between the K^- and the z-axis in the $\bar{K}^*$ rest frame, and ϕ is the angle between the normals to the $\mu^+\mu^-$ and $K\pi$ decay planes in the $\bar{B}$ rest frame. In the case of the B, the angles are defined relative to the μ^+ and the K^+.

The kinematics of the decay is described by three angles, θ_l, θ_K, and ϕ, and the invariant mass squared of the muon pair, q^2. The decay angles are shown in Fig. 1 and defined in its caption. A widely-studied observable is the di-lepton forward-backward asymmetry [5],

$$A_{\rm FB}(q^2) = \frac{\int_0^1 \frac{\partial^2\Gamma}{\partial q^2 \partial\cos\theta_l}\,{\rm d}\cos\theta_l - \int_{-1}^0 \frac{\partial^2\Gamma}{\partial q^2 \partial\cos\theta_l}\,{\rm d}\cos\theta_l}{\int_0^1 \frac{\partial^2\Gamma}{\partial q^2 \partial\cos\theta_l}\,{\rm d}\cos\theta_l + \int_{-1}^0 \frac{\partial^2\Gamma}{\partial q^2 \partial\cos\theta_l}\,{\rm d}\cos\theta_l}. \tag{1.1}$$

The value of q^2 for which $A_{\rm FB}(q^2)$ is 0, known as the zero-crossing point, $q_0^2(A_{\rm FB})$, has reduced hadronic uncertainties due to leading order form-factor (FF) cancellations [6].

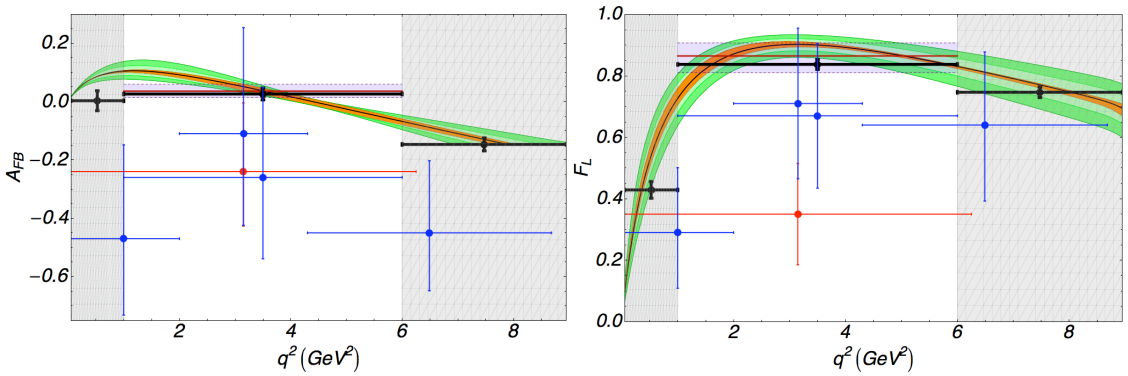

Figure 2: Recent results from *BABAR* (red) and BELLE (blue) for $A_{\rm FB}$ (left) and $F_{\rm L}$ (right) as a function of q^2, re-drawn from Refs. [7]. SM theoretical predictions are shown; the orange, light green, and dark green bands show the parametric and estimated 5% and 10% contributions from unknown higher order terms in the $1/m_b$ expansion, known as Λ/m_b corrections [4]. The light purple bands show the rate-weighted [8] SM average in the region $q^2 \in [1\,\text{GeV}^2, 6\,\text{GeV}^2]$, with all uncertainties. The black points show LHC*b* $2\,\text{fb}^{-1}$ sensitivities using a simultaneous angular projection fit, following Ref. [9] and assuming the SM, where the central value is taken from a single toy experiment.

The SM distributions for $A_{\rm FB}$ and $F_{\rm L}$, the longtitudinal polarization fraction of the $\bar{K}^*$, can be seen in Fig. 2; theoretical uncertainties are not well controlled outside of the $q^2 \in [1\,\text{GeV}^2, 6\,\text{GeV}^2]$ region [2, 4, 10]. Measurements from both *BABAR* and BELLE [7] are shown for points that lie inside this theoretically clean region. For comparison, the $A_{\rm FB}$ distributions for a number of NP models are shown in Fig. 3 (left). The current experimental uncertainties for both $A_{\rm FB}$ and $F_{\rm L}$ are still too large to make any definitive statements about deviations from the SM. The large increase in statistics from LHC*b* will clarify this situation; the estimated sensitivities for LHC*b* with $2\,\text{fb}^{-1}$ of integrated luminosity are shown as the black points in Fig. 2.

2. Physics Programme

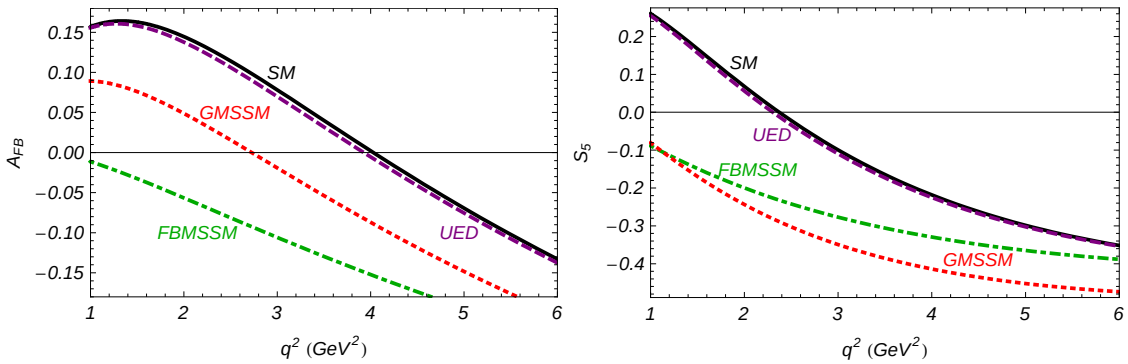

Figure 3: Theoretical $A_{\rm FB}$ and S_5 distributions in a number of models, re-drawn from Ref. [10]. The solid lines give the SM prediction. The dashed lines show predictions from a universal extra dimensions (UED) model, a non-minimal flavour violating supersymmetric model (GMSSM) and a flavour blind supersymmetric model (FBMSSM).

Making precision B-physics measurements in the LHC environment will be challenging but LHC*b* has been carefully optimized to make this possible [1]. The detector is expected to collect $6200\ ^{+1700}_{-1500}$ $B_d \to K^{*0}\mu^+\mu^-$ signal events with 1550 ± 310 background events for each nominal year of data taking ($2\,\text{fb}^{-1}$) [11]. The dominant uncertainty on this yield estimate comes from the branching fraction, which is currently known to an accuracy of $\sim 15\%$ [12]. The large increase in statistics at LHC*b* relative to the previous generation of experiments allows for an ambitious physics programme to be undertaken [13]. A selection of measurements of the angular distribution are discussed below.

2.1 Measuring A_{FB}

The first major analysis target is to map out the A_{FB} distribution and determine $q_0^2(A_{\text{FB}})$. This measurement can be made with relatively low integrated luminosity by counting the number of signal events in angular bins of θ_l to determine A_{FB}, following Eq. (1.1). An example of this is shown in Fig. 4 (left). Taking a particular FF model [14], this approach gives a projected uncertainty of $\sigma(q_0^2(A_{\text{FB}})) = 0.46\,\text{GeV}^2$ for $2\,\text{fb}^{-1}$ of integrated luminosity [15]. However, the uncertainty is approximately proportional to the *gradient* of the A_{FB} distribution, which is in turn dependent on the FFs found in nature; the actual experimental uncertainty found may differ from this estimate as the FFs are not well known.

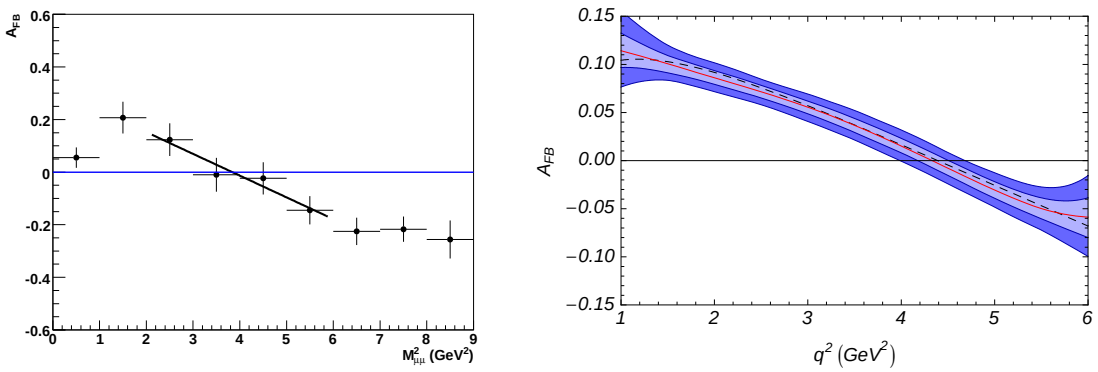

Figure 4: Left: Counting the number of forward and backwards signal events to determine A_{FB} with $2\,\text{fb}^{-1}$ of integrated luminosity [15]. The data-set used was produced with the full LHC*b* detector simulation and a SM signal simulation following Ref. [14] ($M^2_{\mu\mu} \equiv q^2$). A straight-line fit is used to extract $q_0^2(A_{\text{FB}})$. **Right:** Estimated sensitivity to A_{FB} in the range $q^2 \in [1\,\text{GeV}^2, 6\,\text{GeV}^2]$ as extracted using a full angular analysis to $10\,\text{fb}^{-1}$ of toy Monte Carlo LHC*b* data, with the SM signal simulation following Refs. [2, 4]. The dashed black line shows the input SM distribution, while the solid red line is the median of a thousand toy fits. The 1σ and 2σ confidence levels are marked by the light and dark blue bands. The differing input calculations and FF distributions lead to the variations in gradient and $q_0^2(A_{\text{FB}})$ between the two figures.

A particular challenge of making the A_{FB} measurement will be dealing with detector and selection acceptance effects, particularly at low q^2. While a measurement of $q_0^2(A_{\text{FB}})$ should be safe from biases due to these, the rest of the A_{FB} distribution can experience considerable distortion, leading to a systematic effect on $\sigma(q_0^2(A_{\text{FB}}))$ from the change in the A_{FB} gradient induced. These effects must be controlled to an accuracy of $\sim 10\%$ if their contribution to the final uncertainty is to be small [13]. Fig. 5 (left) shows the effects on the θ_l efficiency of the LHC*b* detector geometry

and reconstruction in the low q^2 region, $q^2 \in [1\,\text{GeV}^2, 2\,\text{GeV}^2]$. Many more events with θ_l close to 0 or π are lost than those with θ_l close to $\pi/2$. In the former configuration, $\theta_l[0,\pi]$, events typically feature one high p_T and one low p_T muon; at low q^2 the lower momentum μ often fails to reach the muon chambers and is not reconstructed.

The events with $\theta_l[0,\pi]$ are particularly important for the A_{FB} analysis, as they will show the largest asymmetry in θ_l, and are expected to be produced much less frequently than those with $\theta_l \approx \pi/2$. Fig. 5 (middle) shows the effect of introducing a 300 MeV p_T cut on both muons. In this case the effect is disastrous; the vast majority of these significant events are lost. While these effects are less important at higher q^2, considerable care must be taken to avoid producing these kind of effects in the theoretically clean region. Fig. 5 (right) shows the effect of the LHC*b* trigger and offline selections on a sample of fully simulated signal events. It can be seen that there is little distortion introduced; the main source of acceptance effects is expected to be from the detector geometry and reconstruction.

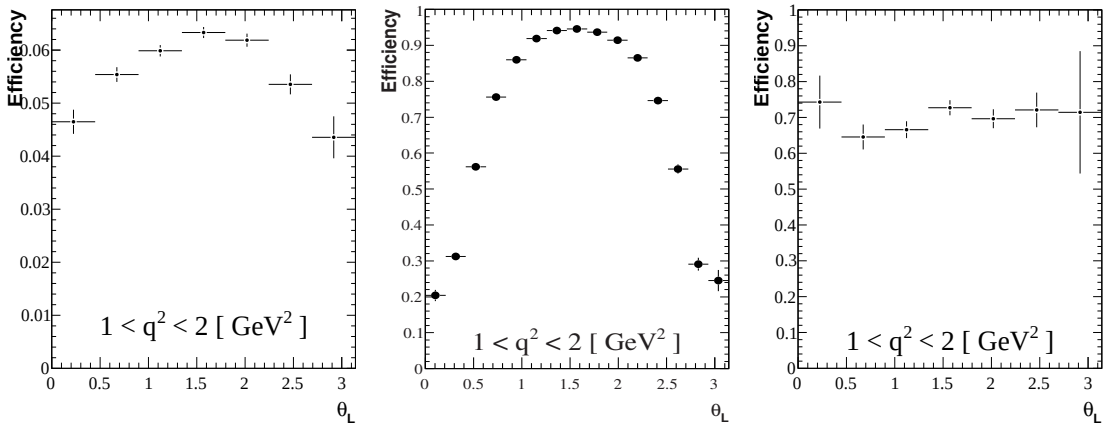

Figure 5: Left: The effect of the detector geometry and reconstruction on the signal selection efficiency as a function of θ_l found from a full detector simulation. **Middle:** The effect of requiring that both muons have a $p_T > 300\,\text{MeV}$ on the signal selection efficiency using a generator-level simulation of the decay kinematics. **Right:** The total effect on the signal selection efficiency from the complete trigger chain, relative to the detector geometry and reconstruction, found from a full detector and trigger simulation.

2.2 Beyond A_{FB}

Measurements involving the counting of signal events as a function of θ_l are attractive as they require a relatively modest understanding of the detector and backgrounds. However, there is much more information available in the decay which can be extracted at the price of a more challenging analysis. These measurements are important as they are complementary to A_{FB} and provide sensitivity to Wilson coefficients beyond $\mathscr{C}_7$ and $\mathscr{C}_9$. Projections of the full angular distribution can be used to perform a simultaneous fit to the decay angles [9]. This gives additional sensitivity to A_{FB} and F_{L}, as shown in Fig. 2, and to non-SM values of $\mathscr{C}_7'$ via a new observable, $A_T^{(2)}$ [3, 16]. Sensitivity to $\mathscr{C}_7'$ may also be gained via the observable S_5 [10], theoretical distributions for which are shown in Fig. 3 (right). S_5 features a zero-crossing point, the measurement of which may be attractive experimentally due to the steep gradient at this point for SM-like scenarios [17]. S_5 may

be extracted by counting the number of signal events as function of the decay angles θ_K and ϕ, using the expression

$$S_5 = \frac{4}{3}\left[\int_0^{\pi/2} + \int_{3\pi/2}^{2\pi} - \int_{\pi/2}^{3\pi/2}\right]\partial\phi\left[\int_0^1 - \int_{-1}^0\right]\partial\cos\theta_K \frac{\partial^3\Gamma}{\partial q^2\partial\phi\partial\cos\theta_K}\Big/\frac{\partial\Gamma}{\partial q^2}; \qquad (2.1)$$

however, controlling acceptance effects in the two angles will be a challenge.

Finally, it is possible to perform a full angular analysis [4, 18]. In this case all four experimental measurables are utilized to extract the underlying decay amplitudes. This allows for the measurement of additional observables which cannot be accessed in other ways. Fig. 6 shows the estimated LHC*b* sensitivity to the theoretically clean observables $A_T^{(3)}$ and $A_T^{(4)}$ for a simulated $10\,\text{fb}^{-1}$ data-set. In addition, significant improvement can be gained on A_{FB} and $q_0^2(A_{\text{FB}})$. Fig. 4 (right) shows the expected sensitivity to A_{FB} with $10\,\text{fb}^{-1}$ of integrated luminosity, giving $\sigma(q_0^2) = {}^{+0.18}_{-0.16}\,\text{GeV}^2$. A further factor of two improvement might be expected if the FF model from [14] had been used instead of that from [2], due the increase in the gradient at $q_0^2(A_{\text{FB}})$. This gradient change may be seen by comparing the central values of the right- and left-hand plots in Fig. 4 and is further explored in Ref. [18].

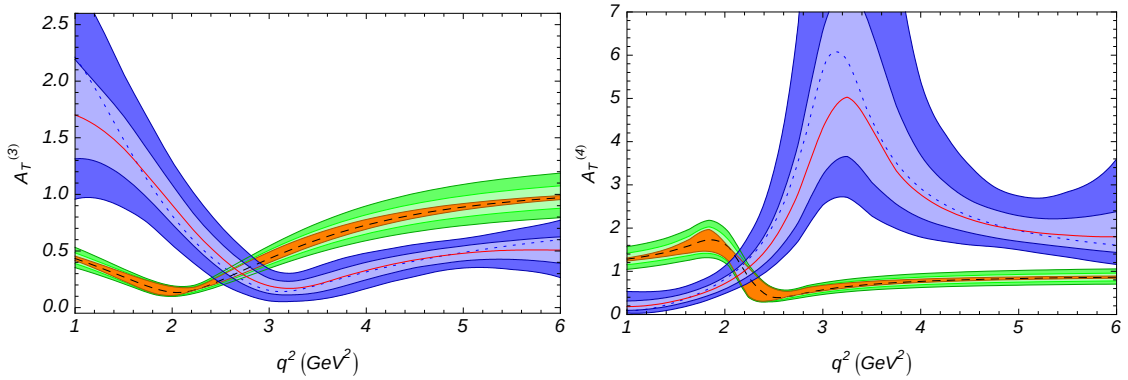

Figure 6: Experimental sensitivity bands (1σ and 2σ uncertainties are marked light and dark blue) for the theoretically clean observables $A_T^{(3)}$ and $A_T^{(4)}$ for $10\,\text{fb}^{-1}$ of LHC*b* data assuming a supersymmetric model [4, 16]. The dashed blue line shows the distribution taken as input, while the solid red line is the median of a thousand toy fits. The SM theoretical distributions are also shown with the same colour scheme as in Fig. 2. These two distributions must be statistically distinguishable if an observation of NP is to be made.

2.3 *CP*-Violation

LHC*b* reconstructs $\bar{B}_d \to \bar{K}^{*0}\mu^+\mu^-$ through the charged decays of the $\bar{K}^{*0}$ so the sign of the K tags the B flavour. Both model dependent [10] and model independent [19] considerations indicate that significant non-SM-like *CP*-violation is possible in the decay though the addition of complex phases in the Wilson coefficients. These remain poorly constrained and could in principle provide a source of *CP*-violation beyond the CKM mechanism. The SM contribution of *CP*-violation is very small, coming from doubly-Cabibbo suppressed diagrams; any *CP*-violation seen in this decay would be a robust sign of NP. Furthermore, the transformation of some parts of the angular distribution under T-parity means that q^2-integrated measurements can be made without separating the data into B and $\bar{B}$ samples [19]. Fig. 7 shows some model-independent predictions for the

angular asymmetry A_8, defined in Ref. [10], and the estimated sensitivity using a full angular analysis. It is clear that more work is required before these sort of measurements become competitive for anything other than very large NP phases. In the case of a full angular analysis, other more theoretically clean observables may also be considered [20].

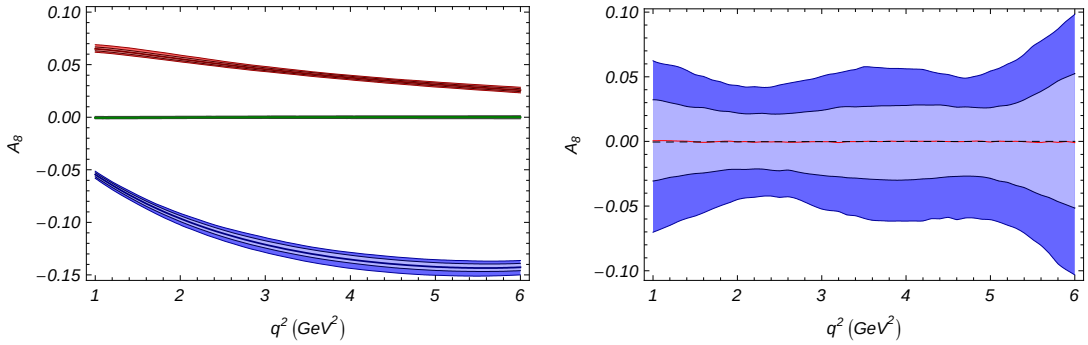

Figure 7: Left: Model-independent distributions for the *CP* asymmetry in the angular component I_8 (A_8) for the SM (green) and NP with $\mathscr{C}_{9\mathrm{NP}} = 2e^{i3\pi/4}$ (red), $\mathscr{C}_{10\mathrm{NP}} = 2e^{i3\pi/4}$ (grey), and $\mathscr{C}'_{10} = 3e^{i3\pi/4}$ (blue). The error bands show estimated Λ/m_b corrections [20] however other theoretical uncertainties are not shown. **Right:** Estimated experimental sensitivity to A_8 after performing a full angular fit to the B and $\bar{B}$ samples assuming the SM for $10\,\mathrm{fb}^{-1}$ of LHC*b* data [20]. The bands have the same meaning as in Fig. 6.

Acknowledgments

The author would like to thank the conference organizers for the convivial atmosphere created and also A. Bharucha, U. Egede, T. Hurth, J. Matias, and M. Ramon for many helpful discussions and stimulating collaborations.

References

[1] **LHC*b*** Collaboration, A. A. Alves *et. al.*, *The LHC*b *Detector at the LHC*, *JINST* **3** (2008) S08005.

[2] M. Beneke, T. Feldmann and D. Seidel, *Systematic approach to exclusive $B \to V l^+ l^-, V\gamma$ decays*, *Nucl. Phys.* **B612** (2001) 25–58 [hep-ph/0106067]; M. Beneke, T. Feldmann and D. Seidel, *Exclusive radiative and electroweak $b \to d$ and $b \to s$ penguin decays at NLO*, *Eur. Phys. J.* **C41** (2005) 173–188 [hep-ph/0412400].

[3] F. Kruger and J. Matias, *Probing new physics via the transverse amplitudes of $B^0 \to K^{*0}(\to K^-\pi^+)l^+l^-$ at large recoil*, *Phys. Rev.* **D71** (2005) 094009 [hep-ph/0502060].

[4] U. Egede, T. Hurth, J. Matias, M. Ramon and W. Reece, *New observables in the decay mode $\bar{B}_d \to \bar{K}^{*0}\mu^+\mu^-$*, *JHEP* **11** (2008) 032 [0807.2589].

[5] A. Ali, T. Mannel and T. Morozumi, *Forward backward asymmetry of dilepton angular distribution in the decay $b \to s l^+ l^-$*, *Phys. Lett.* **B273** (1991) 505–512.

[6] G. Burdman, *Short distance coefficients and the vanishing of the lepton asymmetry in* $B \to V l^+ l^-$, *Phys. Rev.* **D57** (1998) 4254–4257 [hep-ph/9710550].

[7] ***BABAR*** Collaboration, B. Aubert *et. al.*, *Angular distributions in the decays* $B \to K^* l^+ l^-$, *Phys. Rev.* **D79** (2009) 031102 [0804.4412]; **BELLE** Collaboration, J. T. Wei *et. al.*, *Measurement of the differential branching fraction and forward-backword asymmetry for* $B \to K^{(*)} l^+ l^-$, *Phys. Rev. Lett.* **103** (2009) 171801 [0904.0770].

[8] i.e. $\langle \mathscr{O} \rangle_{[q^2_{\rm min}, q^2_{\rm max}]} = \int_{q^2_{\rm min}}^{q^2_{\rm max}} {\rm d}q^2 \left(\mathscr{O}(q^2) \frac{{\rm d}\Gamma}{{\rm d}q^2} \right) \Big/ \int_{q^2_{\rm min}}^{q^2_{\rm max}} {\rm d}q^2 \frac{{\rm d}\Gamma}{{\rm d}q^2}$ for an observable $\mathscr{O}(q^2)$.

[9] U. Egede, "Angular correlations in the $\bar{B}_d \to \bar{K}^{*0}\mu^+\mu^-$ decay." CERN-LHCb-2007-057.

[10] W. Altmannshofer *et. al.*, *Symmetries and asymmetries of* $B \to K^{*0}\mu^+\mu^-$ *decays in the Standard Model and beyond*, *JHEP* **01** (2009) 019 [0811.1214].

[11] J. Dickens, V. Gibson, C. Lazzeroni and M. Patel, "Selection of the decay $B_d \to K^{*0}\mu^+\mu^-$ at LHC*b*." CERN-LHCb-2007-038; M. Patel and H. Skottowe, "A Fisher discriminant selection for $B_d \to K^{*0}\mu^+\mu^-$." CERN-LHCb-2009-009.

[12] **Particle Data Group** Collaboration, C. Amsler *et. al.*, *Review of particle physics*, *Phys. Lett.* **B667** (2008) 1.

[13] **LHC*b*** Collaboration, B. Adeva *et. al.*, *Roadmap for selected key measurements of LHC*b, 0912.4179.

[14] A. Ali, P. Ball, L. T. Handoko and G. Hiller, *A comparative study of the decays* $B \to (K, K^*) l^+ l^-$ *in Standard Model and supersymmetric theories*, *Phys. Rev.* **D61** (2000) 074024 [hep-ph/9910221].

[15] J. Dickens, V. Gibson, C. Lazzeroni and M. Patel, "A study of the sensitivity to the forward-backward asymmetry in $B_d \to K^{*0}\mu^+\mu^-$ decays at LHC*b*." CERN-LHCb-2007-039.

[16] E. Lunghi and J. Matias, *Huge right-handed current effects in* $B \to K^*(K\pi) l^+ l^-$ *in supersymmetry*, *JHEP* **04** (2007) 058 [hep-ph/0612166].

[17] A. Bharucha and W. Reece, *Constraining new physics with* $B_d \to K^{*0}\mu^+\mu^-$ *in the early LHC era*, 1002.4310.

[18] W. Reece and U. Egede, "Performing the full angular analysis of $\bar{B}_d \to \bar{K}^{*0}\mu^+\mu^-$ at LHC*b*." CERN-LHCb-2008-041.

[19] C. Bobeth, G. Hiller and G. Piranishvili, *CP asymmetries in* $\bar{B} \to \bar{K}^{*0}(\to \bar{K}\pi) l^+ l^-$ *and untagged* $\bar{B}_s, B_s \to \phi(\to K^- K^+) l^+ l^-$ *decays at NLO*, *JHEP* **07** (2008) 106 [0805.2525].

[20] U. Egede, T. Hurth, J. Matias, M. Ramon and W. Reece, *The exclusive* $B \to K^{*0}(\to K\pi) l^+ l^-$ *decay: CP–conserving observables*, 0912.1339; U. Egede, T. Hurth, J. Matias, M. Ramon and W. Reece, *New physics reach of CP violating observables in the decay* $B \to K^{*0} l^+ l^-$, 0912.1349; U. Egede, T. Hurth, J. Matias, M. Ramon and W. Reece. In preparation.